

Investigating the parity of the exotic Θ^+ baryon from the kaon photoproduction

Byung-Geel Yu,^{1,2,*} Tae-Keun Choi,^{3,†} and Chueng-Ryong Ji^{2,‡}

¹*Department of General studies, Hangkong Aviation University, Koyang, 200-1, Korea*

²*Department of Physics, North Carolina State University,
Raleigh, North Carolina 27695-8202, USA*

³*Department of Physics, Yonsei University, Wonju, 220-710, Korea*

(Dated: December 26, 2018)

Abstract

Based on the hadronic model with an improved version of gauge prescription including form factors, we investigate the possibility of determining the parity state of Θ^+ baryon using photon induced processes, $\gamma n \rightarrow K^- \Theta^+$, $\gamma p \rightarrow \bar{K}^0 \Theta^+$. The total and differential cross sections are simulated in two versions of pseudovector(PV) and pseudoscalar(PS) coupling schemes for $KN\Theta$ interaction and the results are reported both on the positive and negative parity states of Θ^+ baryon. It is found that in both schemes the total cross sections from the neutron are larger than those from the proton. In particular, not only the cross sections of the positive parity Θ^+ production but also those of the negative parity Θ^+ production are found to be comparable to the cross section observed in the SAPHIR experiment. Our analysis suggests that the observation of angular distribution rather than just the total cross section in the photoproduction processes may be a useful tool to distinguish the parity of Θ^+ baryon.

PACS numbers: 13.60.Rj, 13.60.-r, 13.75.Jz, 14.20.-c

*Electronic address: bgyu@mail.hangkong.ac.kr

†Electronic address: tkchoi@dragon.yonsei.ac.kr

‡Electronic address: crji@unity.ncsu.edu

I. INTRODUCTION

The recent experimental observations of the narrow baryon state from the invariant mass spectrum of K^+n or K^0p in photon induced nuclear reactions and their interpretation as an exotic pentaquark state of Θ^+ baryon with $s=+1$ attracted a lot of attention [1, 2, 3]. Such an experimental evidence for the Θ^+ baryon was also observed in other reaction channels $K^+Xe \rightarrow K^0pXe'$ [4] and $\nu_{\mu^-}(\bar{\nu}_{\mu^-})$ collisions with nuclei [5], which tends to confirm the existence of the Θ^+ baryon. The extracted mass of the Θ^+ baryon from these experiments is reported to be 1.54 GeV and its decay width less than 25 MeV are consistent with those of the pentaquark state predicted in the chiral soliton model [6, 7, 8, 9]. These experimental identification of Θ^+ have initiated intense studies of the new type of hadron structures that are containing more than two or three quarks [10, 11]. However, since quantum numbers other than its mass and decay width of the detected Θ^+ baryon are not yet known from these experiments, much theoretical attention has been paid to the determination of its further properties like spin, isospin, parity and its magnetic moment. Subsequent theoretical investigations on the structure of Θ^+ baryon follow based on the constituent quark model including diquark-diquark- \bar{q} approach [12, 13, 14, 15, 16, 17, 18], Skyrme model [7, 8, 9, 19, 20, 21, 22, 23], QCD sum rule [24, 25, 26], chiral potential model [27], large N_c QCD [28], lattice QCD [29, 30] and Group theory approach [31, 32]. The dynamical properties of Θ^+ baryon was also studied through the production of Θ^+ in the relativistic nuclear collisions [33, 34]. All these theoretical studies address various aspects of the Θ^+ baryon properties and in many cases the models assume or predict a definite parity for the Θ^+ as positive [6, 13, 14, 15, 17, 18, 21, 25, 27]. However, recent works from the QCD-sum rules [24, 26] and the lattice QCD [29, 30] favor a negative parity. Therefore the assumptions based on or the model predictions for the parity of Θ^+ are still controversial and it is thus of importance to analyze the processes that may reveal the true parity state of the Θ^+ . Along this line of thoughts, there are theoretical attempts to determine the parity of Θ^+ baryon by the direct estimation of the cross sections observed in the photon and meson induced Θ^+ production experiments [35, 36, 38, 39, 40]. In these works, we see that some of these hadronic models incorporate hadron form factors in order to cut off the divergence of the cross sections at high energy and estimate the cross sections of $\gamma n \rightarrow K^-\Theta^+$ and $\gamma p \rightarrow \bar{K}^0\Theta^+$ to compare with the observed cross section in the SAPHIR experiment [36, 38]. However, none of these predictions are made on the broader basis of a consistent treatment of gauge invariance when the form factors are incorporated, as we will discuss in this work. In Ref. [38], although several improvements are found, the model calculation still needs further improvement in the sense

that the gauge prescription they used for the hadron form factors is lacking somewhat broader basis of theoretical justification at least within the tree level hadron models. This point cannot be overlooked from the knowledges of the similar processes, $\gamma p \rightarrow K^+ \Lambda$ and $\gamma p \rightarrow K^+ \Sigma^0$, where the consistent treatment of form factors based on the more reliable prescription for gauge invariance is indispensable [41, 42, 43, 44], since it could affect largely the model parameters, and as a consequence alter the theoretical predictions to a large extent.

Motivated by the theoretical importance of the processes $\gamma n \rightarrow K^- \Theta^+$ and $\gamma p \rightarrow \bar{K}^0 \Theta^+$ to study the structure of the Θ^+ baryon and the necessity to improve the existing calculations on these processes, we perform more elaborate and consistent calculations of total and differential cross sections for these reactions. Our primary interest here is to investigate the possibility of discriminating the parity of Θ^+ baryon using these processes and, further, aim at providing reliable results of the cross sections that will be utilized for the future theoretical and experimental studies relevant to the Θ^+ baryon. For this purpose, we will stress the advantage of using the angular distribution of the reaction rather than just using the total cross section. While the magnitude of the total cross section depends on the choice of form factors together with the variation of cutoff parameter Λ , the features of angular distribution following the conservation rules of parity and angular momentum are less dependent on such model parameters.

This paper is organized as follows. In Sec. II, the cross section and the differential cross section for angular distribution are evaluated for Θ^+ production from $\gamma N \rightarrow K \Theta^+$ when Θ^+ has positive parity. The cross section and angular distribution of the reaction in the case of the negative parity Θ^+ production are evaluated in Sec. III. Summary and discussion follow in Sec. IV.

II. PHOTOPRODUCTION FOR POSITIVE PARITY Θ^+

The photoproduction of the Θ^+ baryon from neutron and proton targets is usually calculated in relativistic hadron models because the models with hadronic degrees of freedom are more relevant than the perturbative QCD to the energy range of the reactions that we study in this work. In hadronic models the reaction is generated from the Feynman diagrams at tree level as shown in Fig. 1. The momenta of the incident photon, the nucleon, the outgoing K , and Θ are k , p , q , and p' , respectively in the diagrams of Fig. 1. The Mandelstam variables are $s = (p + k)^2$, $t = (k - q)^2$, and $u = (p' - k)^2$. Using effective Lagrangians for vertex couplings pertinent to the diagrams, the transition amplitude is obtained. Here, as the interaction Lagrangians relevant to the process are found in many literatures [36, 37, 38, 40] we will not repeat them. Instead, with the interaction

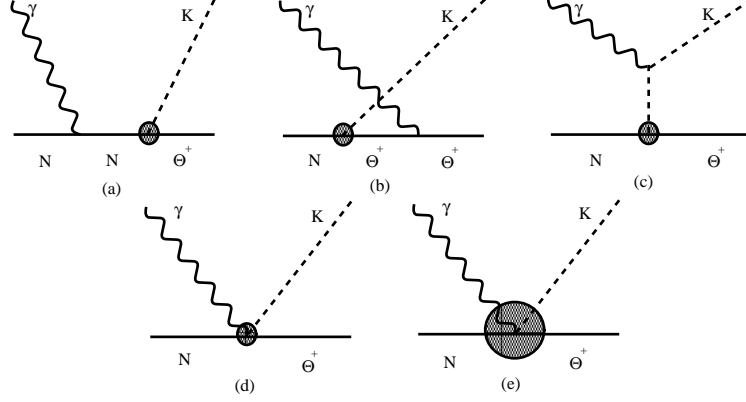


FIG. 1: Tree level diagrams for $\gamma N \rightarrow K\Theta^+$ reaction. Diagrams (a), (b) and (c) denote the s-, u- and t-channel pole terms with hadron form factors depicted as blobs at each vertex. The diagram (d) is the Kroll-Ruderman(KR) term; it is absent for pseudoscalar couplings with bare vertices. The last diagram (e) corresponds to the contact interaction term required to restore gauge invariance of Born amplitude. It is depicted as a large blob to distinguish from the KR term.

Lagrangians given in Refs. [36, 38], let us begin with the Born amplitude for the positive parity Θ^+ photoproduction,

$$\mathcal{M}_{Born} = \mathcal{M}_{PV-pole} + \mathcal{M}_{KR} + \mathcal{M}_c. \quad (1)$$

The PV-pole terms are composed of s-, u- and t-channel, nucleon, Θ^+ and kaon exchanges corresponding to the first three pole diagrams of (a), (b) and (c) in Fig. 1, i.e.,

$$\begin{aligned} & \mathcal{M}_{PV-pole} \\ &= \frac{eg_{KN\Theta}}{M + M_\Theta} \bar{u}_\Theta(p') \left\{ F_1(s) \gamma_5 \not{\epsilon} \frac{(\not{p} + \not{k} + M)}{s - M^2} [Q_N \not{\epsilon} + i \frac{\kappa_N}{2M} \sigma^{\mu\nu} \epsilon_\mu k_\nu] + [Q_\Theta \not{\epsilon} + i \frac{\kappa_\Theta}{2M_\Theta} \sigma^{\mu\nu} \epsilon_\mu k_\nu] \right. \\ & \times \frac{(\not{p}' - \not{k} + M_\Theta)}{u - M_\Theta^2} \gamma_5 \not{\epsilon} F_2(u) + Q_K F_3(t) \gamma_5 (M + M_\Theta) \frac{(2q - k) \cdot \epsilon}{t - m_K^2} \left. \right\} u_N(p). \end{aligned} \quad (2)$$

For brevity, we write the amplitude collectively for $\gamma n \rightarrow K^- \Theta^+$ and $\gamma p \rightarrow \bar{K}^0 \Theta^+$ with notations Q_N , Q_Θ and Q_K by assigning $Q_N = 0$, $Q_\Theta = 1$ and $Q_K = -1$ to $\gamma n \rightarrow K^- \Theta^+$, and $Q_N = 1$, $Q_\Theta = 1$ and $Q_K = 0$ to $\gamma p \rightarrow \bar{K}^0 \Theta^+$, respectively. The anomalous magnetic moments of the proton and neutron are $\kappa_p = 1.79$ and $\kappa_n = -1.91$. In Eq.(2), $g_{KN\Theta}$ is the Θ^+ coupling constant, κ_Θ is the anomalous magnetic moment of Θ^+ , and ϵ is the photon polarization vector. Also, $F_1(s) = F_1(s, M'^2, m_\pi^2)$, $F_2(u) = F_2(M^2, u, m_\pi^2)$ and $F_3(t) = F_3(M^2, M'^2, t)$ are the hadron form factors introduced to s-, u- and t-channel $KN\Theta$ coupling vertices with the normalizations $F_1(s = M^2) = 1$, $F_2(u = M'^2) = 1$ and $F_3(t = m_\pi^2) = 1$, respectively. In PV coupling, the Kroll-Ruderman term of

Fig. 1 (d) is required to restore gauge invariance of PV pole terms due to the $\gamma_5 \not{\epsilon}$ coupling;

$$\mathcal{M}_{KR} = -\frac{eg_{KN\Theta}}{M + M_\Theta} \bar{u}_\Theta(p') \gamma_5 \not{\epsilon} \left\{ F_1(s) Q_N - Q_\Theta F_2(u) \right\} u_N(p). \quad (3)$$

In the gauge transformation of the PV coupling pole terms together with the Kroll-Ruderman term, however, these amplitudes are not gauge invariant, but yield the following relation,

$$(\mathcal{M}_{PV-pole} + \mathcal{M}_{KR})_{\epsilon \rightarrow k} = eg_{KN\Theta} \bar{u}_\Theta(p') \gamma_5 \left\{ F_1(s) Q_N - Q_\Theta F_2(u) - Q_K F_3(t) \right\} u_N(p). \quad (4)$$

The nonvanishing divergence of Eq.(4) is due to the different form factors and this equally holds for the gauge transformation of PS coupling photoproduction amplitude. In fact it vanishes when $F_i = 1$ for $i = 1, 2, 3$, i.e., in the case of point interaction of $KN\Theta$, or when $F_i = F$ for all i , i.e., in the case of using an overall form factor, F . In Refs. [36, 38] the recipe they used in order to restore gauge invariance of the Born amplitude as given in Eq.(4) corresponds to the case of using an overall form factor. In this work, we note that the more elaborate prescription consistent with the field theoretic approach is given by Ohta [45] and later improved further by Haberzettl [46]. According to these field theoretic analysis [45, 46], the divergence of hadronic current due to the different form factors can be removed by introducing the diagram (e) of Fig. 1, so called contact interaction term. It is of the form;

$$\begin{aligned} \mathcal{M}_c = & -eg_{KN\Theta} \bar{u}_\Theta(p') \gamma_5 \left\{ (F_1(s) - \hat{F}) Q_N \frac{(2p+k) \cdot \epsilon}{s - M^2} + Q_\Theta (F_2(u) - \hat{F}) \frac{(2p' - k) \cdot \epsilon}{u - M_\Theta^2} \right. \\ & \left. + Q_K (F_3(t) - \hat{F}) \frac{(2q - k) \cdot \epsilon}{t - m_K^2} \right\} u_N(p). \end{aligned} \quad (5)$$

Here, \hat{F} is a subtraction function which depends on the Mandelstam variables (s, u, t) . In order to maintain the original singularity structure of the Born amplitude, it should be nonsingular, $\hat{F} = 1$, for on-mass shell and preserve the crossing invariance of the reaction [47, 48]. In this work, to preserve the crossing symmetry of the amplitude, we choose the subtraction function, in specific,

$$\hat{F} = F_2(u) + F_3(t) - F_2(u)F_3(t), \quad \hat{F} = F_1(s) + F_2(u) - F_1(s)F_2(u) \quad (6)$$

for $\gamma n \rightarrow K^- \Theta^+$ and $\gamma p \rightarrow \bar{K}^0 \Theta^+$, respectively. For each hadron form factor in the channels $x = s, u, t$, (or $i=1, 2, 3$), we use

$$F_i(x, M_i) = \frac{\Lambda^4}{\Lambda^4 + (x - M_i^2)^2}, \quad (7)$$

which are normalized to unity at $x = M_i^2$. Here M_i is the mass of the exchanged particle and x is the square of the transferred momentum. This function has the correct on-shell condition, i.e., $F_i(x = M_i^2) = 1$ for $i=1, 2, 3$ and, thus, $\hat{F} = 1$ by Eq.(6).

In PS coupling, the Born amplitude is composed of those depicted by Figs. 1(a) - (c). By the similar procedure of including form factors, the Born amplitude which preserves gauge invariance can be obtained by

$$\mathcal{M}_{Born} = \mathcal{M}_{PS-pole} + \mathcal{M}_c, \quad (8)$$

where

$$\begin{aligned} \mathcal{M}_{PS-pole} &= e g_{KN\Theta} \bar{u}_\Theta(p') \left\{ F_1(s) \gamma_5 \frac{(\not{p} + \not{k} + M)}{s - M^2} [Q_N \not{\epsilon} + i \frac{\kappa_N}{2M} \sigma^{\mu\nu} \epsilon_\mu k_\nu] + [Q_\Theta \not{\epsilon} + i \frac{\kappa_\Theta}{2M_\Theta} \sigma^{\mu\nu} \epsilon_\mu k_\nu] \right. \\ &\quad \times \frac{(\not{p}' - \not{k} + M_\Theta)}{u - M_\Theta^2} \gamma_5 F_2(u) + Q_K F_3(t) \gamma_5 \frac{(2q - k) \cdot \epsilon}{t - m_K^2} \left. \right\} u_N(p), \end{aligned} \quad (9)$$

and the contact interaction term of Fig. 1 (e) is given by Eq.(5).

In the calculation of cross sections based on our framework(i.e., Eq.(1) for PV and Eq.(8) for PS coupling scheme of positive parity Θ^+ production), the coupling constant $g_{KN\Theta}$ and the anomalous magnetic moment κ_Θ are to be determined. Unfortunately, there are no detailed informations available on these quantities at present. Instead, we have only few experimental observations; the decay width Γ_Θ and the cross section. It is reported that Γ_Θ is in the range $5 \sim 25$ MeV [1, 2, 3] and the cross section of $\gamma p \rightarrow \bar{K}^0 \Theta^+$ is observed to be on the average a few hundreds of nb in the photon energy range $E_\gamma = 1.75 \sim 2.6$ GeV [2]. In this work, we adopt $g_{KN\Theta}=2.2$ GeV assuming $\Gamma_\Theta < 9$ MeV for positive parity Θ^+ couplings to KN to be consistent with the observed total cross section of $\gamma p \rightarrow \bar{K}^0 \Theta^+$. The value of κ_Θ is still elusive, although there are some theoretical suggestions on this quantity [6, 10]. We consider it as a parameter and vary its value between $-0.7 \leq \kappa_\Theta \leq 0.7$.

The results are shown in Fig. 2. The solid lines are the total cross sections of $\gamma n \rightarrow K^- \Theta^+$ and $\gamma p \rightarrow \bar{K}^0 \Theta^+$ with $g_{KN\Theta} = 2.2$, $\kappa_\Theta = 0$. As can be seen, most of the cross sections are about 200 nb and comparable to the observed values in the SAPHIR experiment as they should be, except the one in the PV scheme(lower left panel in Fig. 2). It should be noted that they are the results of Born contributions only, using Eq.(1) for PV and Eq.(8) for PS scheme, respectively with the form factors given in Eqs.(6) and (7) with the cutoff $\Lambda = 1.8$ GeV $^{-1}$. This point is in sharp contrast to the results of previous calculations. In Ref. [36], with more contributions of the two and three body final state interactions considered, the authors used t-channel and u-channel Born amplitude and obtained cross sections with magnitude 38 nb in $\gamma p \rightarrow \bar{K}^0 \Theta^+$ and 280 nb in $\gamma n \rightarrow K^- \Theta^+$ in the PS scheme. Also in Ref. [38], the authors included K^* exchange in their PS coupling Born

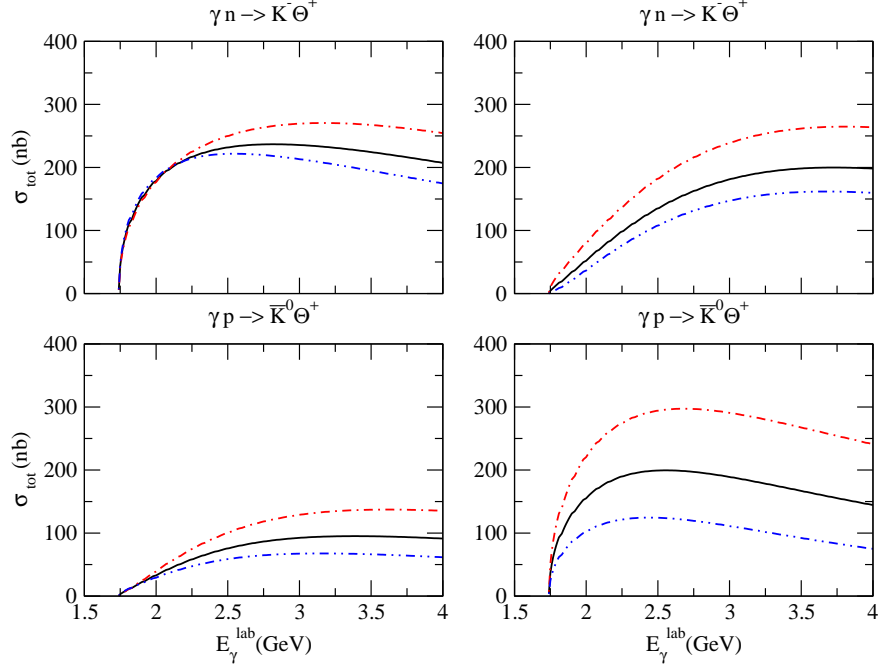


FIG. 2: Cross sections for $\gamma n \rightarrow K^- \Theta^+$ of PV (upper left panel) and PS scheme (upper right panel). Cross sections for $\gamma p \rightarrow \bar{K}^0 \Theta^+$ of PV (lower left panel) and PS scheme (lower right panel). The subtraction function (6) and form factors (7) with cutoff $\Lambda = 1.8$ GeV are used. The solid lines are the results of Born amplitude with $g_{KN\Theta} = 2.2$, $\kappa_\Theta = 0$ when Θ^+ has the positive-parity. The dot-dashed lines are Born contribution with $\kappa_\Theta = 0.7$ and the dot-dot-dashed lines with $\kappa_\Theta = -0.7$.

amplitude to obtain the cross sections with $320 \sim 400$ nb for $\gamma p \rightarrow \bar{K}^0 \Theta^+$ and with $200 \sim 230$ nb for $\gamma n \rightarrow K^- \Theta^+$, depending on the change in the sign of $g_{K^* N \Theta}$. But the Born contributions to these total cross sections are found to be about 40 nb and 80 nb for each process and almost the rest of the cross sections are from K^* contributions. In fact their Born contributions are by a factor of $\frac{1}{3}$ or $\frac{1}{4}$ smaller than our result in PS scheme of Fig. 2, up to $E_\gamma = 4$ GeV. As a consequence, they require such a large contribution of K^* in their calculation. Furthermore, in contrast to their findings in the κ_Θ contributions, we see that the cross sections are significantly dependent on the variation of κ_Θ in the PS scheme, and its contribution is still considerable in the PV scheme, albeit parameterized as the same value with that of Ref. [38]. Besides the different type of form factor used in Ref. [36] from ours and Ref. [38], the apparent distinction between these results and ours are mainly because of the different gauge prescriptions adopted in each model calculation. Although, neither of the procedures adopted in Refs. [36, 38], i.e. taking an overall form factors $F = F_i$ for all i , violates the gauge invariance, we emphasize that, from a field theoretic point of view, it certainly needs further improvement in going beyond just taking

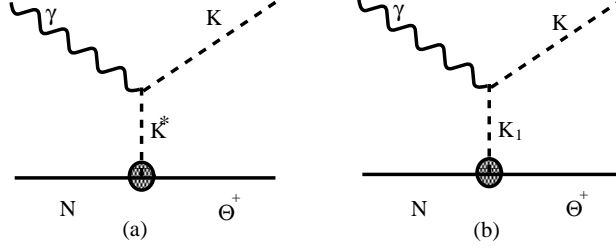


FIG. 3: Diagrams for t-channel K^* and K_1 exchanges in the $\gamma N \rightarrow K \Theta^+$ process.

such a single overall form factor. In Fig. 2, we note that the cross section of $\gamma n \rightarrow K^- \Theta^+$ near threshold is similar to that of $\gamma n \rightarrow \pi^- p$ and also that of $\gamma p \rightarrow \bar{K}^0 \Theta^+$ to $\gamma p \rightarrow \pi^0 p$, since the two channels of Θ^+ production have the same charge exchange structure of Born terms with the corresponding two processes in the pion photoproduction. According to the results of Refs. [49, 50] where the couplings of the baryon octet with the anti-decuplet are analyzed, the couplings of Θ^+ to any would-be nucleon resonances are difficult to occur. We, thus, refer a qualitative analysis of our cross sections to those of the pion photoproduction near threshold where no significant contributions are attributed to the resonances [51]. With these in mind, the "nose" structure of PV coupling scheme of $\gamma n \rightarrow K^- \Theta^+$ near threshold is understood by the Kroll-Ruderman term and possibly the kaon pole term. The Kroll-Ruderman term dictates the threshold amplitude, giving large s-wave contribution to yield a rapid increase of cross section together with the kaon pole term, while for the process $\gamma p \rightarrow \bar{K}^0 \Theta^+$, there is neither Kroll-Ruderman term nor kaon pole term due to the charge conservation. Therefore, the cross section of latter process is suppressed near threshold similar to the case of $\gamma p \rightarrow \pi^0 p$ [52]. These qualitative features are apparent in the PV coupling scheme and consistent with the remark in Ref. [54] that the photoexcitation of the baryon anti-decuplet is strongly suppressed in the proton target and the process occurs mostly in the neutron target. To proceed, we further consider the contributions of t-channel vector meson K^* and K_1 axial vector meson exchanges. Fig. 3 depicts the Feynman diagrams for the K^* and K_1 exchanges in the t-channel. For the $K^*(890)(J^P = 1^-)$ exchange, we use the Lagrangians

$$\begin{aligned} \mathcal{L}_{K^* N \Theta} &= g_{K^* N \Theta} \bar{\Theta} \left(\gamma^\mu + \frac{\kappa^*}{M + M_\Theta} \sigma^{\nu\mu} \partial_\nu \right) K_\mu^* N + \text{h.c.}, \\ \mathcal{L}_{K^* K \gamma} &= \frac{g_{K^* K \gamma}}{m} \epsilon_{\alpha\beta\mu\nu} \partial^\alpha A^\beta \partial^\mu K^\dagger K^{*\nu} + \text{h.c.}, \end{aligned} \quad (10)$$

where $g_{K^* N \Theta}$ and κ^* are respectively the vector coupling constant and the tensor coupling ratio of $K^* N \Theta$ vertex. Here m is a parameter of mass dimension for the anomalous coupling of $g_{K^* K \gamma}$.

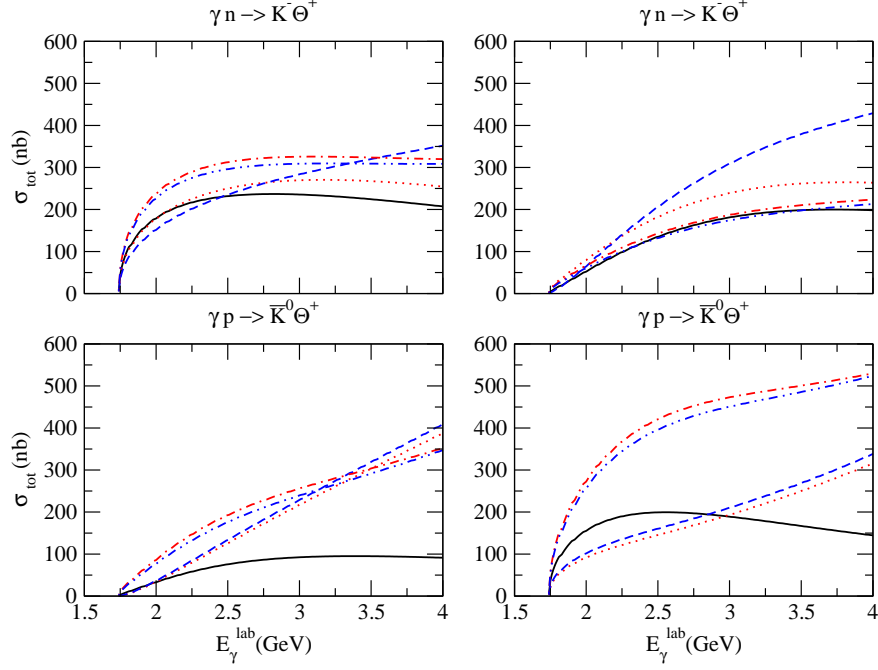


FIG. 4: Cross sections for $\gamma n \rightarrow K^- \Theta^+$ of PV(upper left) and PS scheme(upper right). Cross sections for $\gamma p \rightarrow \bar{K}^0 \Theta^+$ of PV(lower left) and PS scheme(lower right) when the Θ^+ has positive-parity. The subtraction function (6) and form factors (7) with $\Lambda = 1.8$ GeV are used. $\kappa_\Theta = 0$ in any cases for all panels. The solid lines are the contribution of Born amplitude with $g_{K^*N\Theta} = 0$. The dotted lines are the sum of Born terms and K^* with $g_{K^*N\Theta} = 1.32$. The dot-dashed lines the sum of Born terms and K^* with $g_{K^*N\Theta} = -1.32$. The dashed lines are the sum in total of Born terms, K^* and K_1 with $g_{K^*N\Theta} = 1.32$, $g_{K_1N\Theta} = -0.07$ for $\gamma n \rightarrow \bar{K}^0 \Theta^+$ and $g_{K_1N\Theta} = -0.1$ for $\gamma p \rightarrow \bar{K}^0 \Theta^+$ respectively. The dot-dot-dashed lines are the sum in total of Born terms, K^* and K_1 with $g_{K^*N\Theta} = -1.32$, $g_{K_1N\Theta} = +0.07$ for $\gamma n \rightarrow \bar{K}^0 \Theta^+$ and $g_{K_1N\Theta} = +0.1$ for $\gamma p \rightarrow \bar{K}^0 \Theta^+$ respectively.

The transition amplitude for K^* exchange in the t-channel can be written as

$$\mathcal{M}_{K^*} = -G_{K^*N\Theta} \bar{u}_\Theta \left\{ \epsilon_{\alpha\beta\tau\sigma} k^\alpha \epsilon^\beta q^\tau \frac{(-g^{\sigma\mu} + q'^\sigma q'^\mu / M_{K^*}^2)}{t - M_{K^*}^2 + i\Gamma M_{K^*}} \left(\gamma_\mu + i \frac{\kappa^*}{M + M_\Theta} \sigma_{\nu\mu} q'^\nu \right) \right\} u_N, \quad (11)$$

with $G_{K^*N\Theta} = g_{K^*N\Theta} g_{K^*K\gamma} F_3(t) m^{-1}$, and $q'_\mu = (q - k)_\mu$. Including these contributions, we use $g_{K^*K^\pm\gamma} = 0.254$ GeV $^{-1}$ for the charged kaon anomalous decay and $g_{K^*K^0\gamma} = 0.388$ GeV $^{-1}$ for the neutral kaon decay that are cited in PDG [55]. In Ref. [37], the unknown coupling $g_{K^*N\Theta}$ is deduced to be 1.32 from the assumption, $g_{K^*N\Theta}/g_{KN\Theta} = 0.6$. We adopt this value of $g_{K^*N\Theta}$ and in order to avoid further parameters we will not consider the tensor coupling contributions of both K^* and K_1 . The interaction Lagrangians for the axial vector meson $K_1(1270)(J^P = 1^+)$ coupling to $K_1N\Theta^+$ and $K_1K\gamma$ are given by

$$\mathcal{L}_{K_1N\Theta} = g_{K_1N\Theta} \bar{\Theta} \left(\gamma_\mu + \frac{\kappa_1}{M + M_\Theta} \sigma_{\nu\mu} \partial^\nu \right) K_1^{\mu\dagger} \gamma_5 N + \text{h.c.},$$

$$\mathcal{L}_{K_1 K \gamma} = -i \frac{g_{K_1 K \gamma}}{m} K^\dagger (\partial_\mu A_\nu \partial^\mu K_1^\nu - \partial_\mu A_\nu \partial^\nu K_1^\mu) + \text{h.c.}, \quad (12)$$

where $g_{K_1 N \Theta}$ and κ_1 are the axial vector coupling constant and the tensor coupling ratio of $K_1 N \Theta$ vertex, respectively. Then, the transition amplitude for the t-channel K_1 exchange is given by,

$$\mathcal{M}_{K_1} = G_{K_1 N \Theta} \bar{u}_\Theta (k \cdot q' \epsilon_\mu - \epsilon \cdot q' k_\mu) \frac{(-g^{\mu\nu} + q'^\mu q'^\nu / M_{K_1}^2)}{t - M_{K_1}^2 + i\Gamma M_{K_1}} \left(\gamma_\nu + i \frac{\kappa_1}{M + M_\Theta} \sigma_{\alpha\nu} q'^\alpha \right) \gamma_5 u_N, \quad (13)$$

with $G_{K_1 N \Theta} = g_{K_1 N \Theta} g_{K_1 K \gamma} F_3(t) m^{-1}$. For the axial vector meson coupling constant $g_{K_1 K \gamma}$, there are no empirical data available for the decay $K_1 \rightarrow K \gamma$ except for its decay channel to ρ meson via the process $K_1 \rightarrow \rho K$. In Ref. [56], using the effective Lagrangian given by Eq.(12) for the interaction vertex $K_1 K \rho$, its decay width is estimated and the coupling constant $g_{K_1 K \rho}$ is determined to be 12.0 GeV^{-1} from the empirical value $\Gamma_{K_1 \rightarrow K \rho} = 37.8 \text{ MeV}$ [55]. By using the vector dominance relation for $g_{K_1 K \gamma} = \frac{e}{f_\rho} g_{K_1 K \rho}$, the coupling constant $g_{K_1 K \gamma} = 0.6 \text{ GeV}^{-1}$ was then deduced. In order to determine the axial vector coupling constant $g_{K_1 N \Theta}$, we make use of the ratio $g_{K^* K \gamma} g_{K^* p \Lambda} / g_{K_1 K \gamma} g_{K_1 p \Lambda} \simeq -8.6$ extracted from WJC model for $K^+ \Lambda(1116)$ electromagnetic production [57] and assume this ratio is valid also for $g_{K^* K \gamma} g_{K^* N \Theta} / g_{K_1 K \gamma} g_{K_1 N \Theta}$ to obtain $g_{K_1 N \Theta} = -0.07$ for $\gamma n \rightarrow K^- \Theta^+$ and $g_{K_1 N \Theta} = -0.1$ for $\gamma p \rightarrow \bar{K}^0 \Theta^+$, respectively. In Fig. 4, we present the results of K^* and K_1 contributions to cross sections of $\gamma n \rightarrow K^- \Theta^+$ and $\gamma p \rightarrow \bar{K}^0 \Theta^+$ in both coupling schemes. As can be seen, the cross sections are consistent with the observation of SAPHIR collaboration that the mean cross section for $\gamma p \rightarrow \bar{K}^0 \Theta^+$ is in the order of 300 nb, if including the contribution of anomalous magnetic moment κ_Θ shown in Fig. 2. A few comments are in order. In most cases, K^* gives significant contributions, whereas the role of K_1 is minor. As a combined effect, these contributions to $\gamma p \rightarrow \bar{K}^0 \Theta^+$ are dominant over those to $\gamma n \rightarrow K^- \Theta^+$. We also notice that for these reactions, the PV scheme is more stable than the PS scheme when the t-channel K^* and K_1 exchanges are incorporated [58]. However, contrary to the finding of Ref. [38], we could not determine the favorable phase of K^* coupling constant from the present results, since the total cross sections in any cases are comparable to the SAPHIR observation even when the signs of coupling constants $g_{K^* N \Theta}$ and $g_{K_1 N \Theta}$ are changed, as shown in the figures. Instead, we remark that the PV coupling scheme is more favorable for the Θ^+ photoproduction in accordance with the fact that Θ^+ production from the neutron is more active than from the proton.

In Fig. 5, the differential cross sections for $\gamma n \rightarrow K^- \Theta^+$ are displayed near threshold $E_\gamma = 1.8 \text{ GeV}$ and at 2.5 GeV . It is interesting to see that the angular distribution of the produced kaon near threshold, $E_\gamma = 1.8 \text{ GeV}$ is isotropic both in the PV and PS scheme. This is due to the

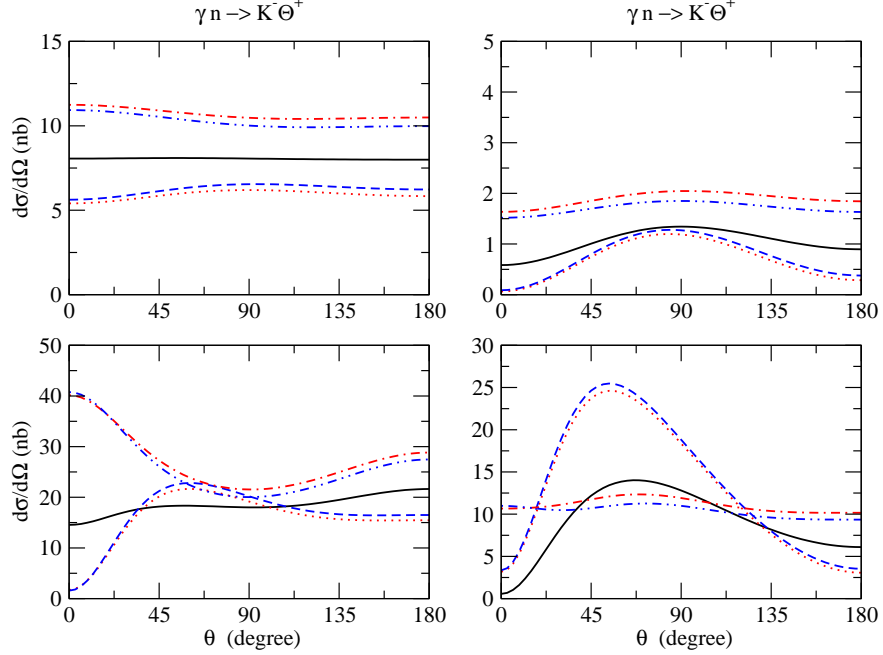


FIG. 5: Photoproduction angular distributions for $\gamma n \rightarrow K^- \Theta^+$ at $E_\gamma = 1.8$ GeV(upper left), $E_\gamma = 2.5$ GeV(lower left) of PV and $E_\gamma = 1.8$ GeV(upper right), $E_\gamma = 2.5$ GeV(lower right) of PS scheme when the parity of Θ^+ is positive. The notations are the same as in Fig. 4

s-wave dominance from the Kroll-Ruderman term in the case of PV, and that from the s-channel in the case of PS, respectively. Notice that the scales of the cross sections in the two schemes are different. This feature of the s wave production near threshold can be anticipated from the parity conservation which states that the produced kaon is in the s-wave near threshold if the parity of Θ^+ is positive. The interference of K^* and K_1 exchanges with Born term entails two possible phases which depend on the change in the sign of their coupling constants. Near threshold, it shows two opposite phases with the coupling constants, $g_{K^*N\Theta} = -1.32$, $g_{K_1N\Theta} = 0.07$ chosen for the dot-dot-dashed lines, and $g_{K^*N\Theta} = 1.32$, $g_{K_1N\Theta} = -0.07$ for the dashed lines. In the energy bin $E_\gamma = 2.5$ GeV, the interference of K^* and K_1 exchanges develops the behavior of the two possible phases very different from each other; the one peak at the very forward angle when $g_{K^*N\Theta} = -1.32$, $g_{K_1N\Theta} = 0.07$, whereas the other peak shifted to be at around 45° when $g_{K^*N\Theta} = 1.32$, $g_{K_1N\Theta} = -0.07$ in the PV scheme(lower left panel). While in the PS scheme a forward peak is observed at around 45° due to the coherent contributions of Born terms with K^* , K_1 with $g_{K^*N\Theta} = 1.32$, $g_{K_1N\Theta} = -0.07$, which is compatible with the result of Ref. [38].

In the angular distributions of $\gamma p \rightarrow \bar{K}^0 \Theta^+$ in Fig. 6, there appear small deviations from the isotropic angular distribution in the Born contribution and the backward asymmetries are

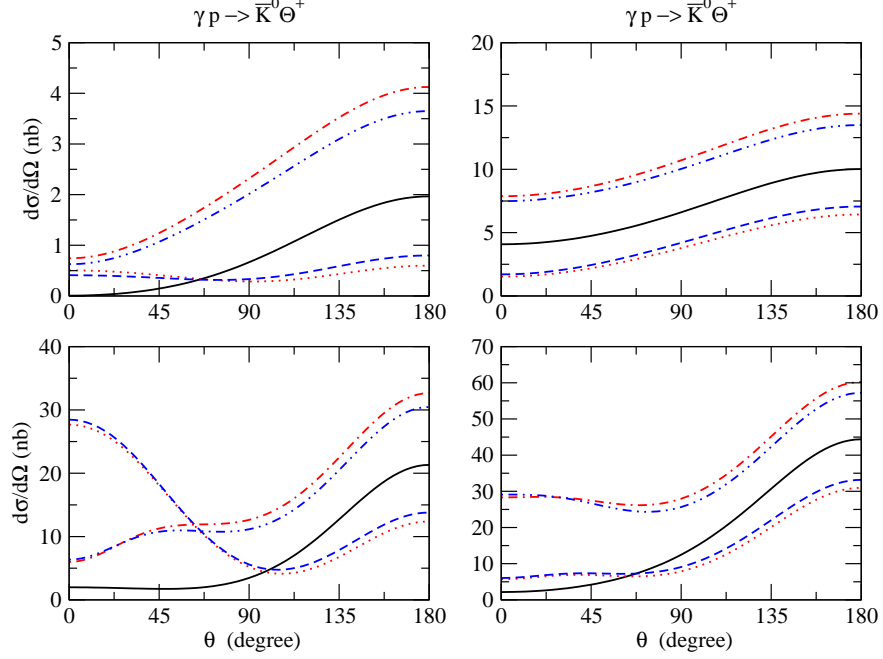


FIG. 6: Photoproduction angular distributions for $\gamma p \rightarrow \bar{K}^0 \Theta^+$ at $E_\gamma = 1.8$ GeV (upper left), $E_\gamma = 2.5$ GeV (lower left) of PV and $E_\gamma = 1.8$ GeV (upper right), $E_\gamma = 2.5$ GeV (lower right) of PS scheme when the parity of Θ^+ is positive. The notations are the same as in Fig. 4

observed near threshold. These backward enhancements hold even at $E_\gamma = 2.5$ GeV both in the PV and PS schemes. They result from the u-channel contribution of the Born term only, since there contributes neither kaon pole term nor Kroll-Ruderman term, which otherwise can give large s-wave contributions. Thus, the angular distribution of u-channel Born contribution manifests the s-wave kaon production in this channel. In practice, the threshold behaviors of Born terms of these two processes show a close similarity to those of $\gamma n \rightarrow \pi^- p$ and $\gamma p \rightarrow \pi^0 p$ near threshold found in Ref. [52, 53], as mentioned before. These figures are also showing that the K^* and K_1 interfere with the Born terms in two opposite ways depending on their coupling constants. At $E_\gamma = 2.5$ GeV we notice again that the change in the sign of K^* and K_1 coupling constants yields the behavior of the two possible phases very different from each other; the one peak at the very forward angle when $g_{K^*N\Theta} = 1.32$, $g_{K_1N\Theta} = -0.1$, and the other at the very backward peak when $g_{K^*N\Theta} = -1.32$, $g_{K_1N\Theta} = 0.1$ in the PV coupling scheme (lower left panel) in Fig. 6. We comment that these characteristics found in the lower left panel in Fig. 5 together with that of Fig. 6 are important, for they may help to determine the correct phases of coupling constants $g_{K^*N\Theta}$ and $g_{K_1N\Theta}$.

III. PHOTOPRODUCTION FOR NEGATIVE PARITY Θ^+

We now turn to the case of Θ^+ photoproduction when it has negative parity. The electromagnetic coupling vertex of the negative parity Θ^+ baryon is given by,

$$\mathcal{L}_{\gamma\Theta\Theta} = -\bar{\Theta}\gamma_5 \left[Q_\Theta \gamma^\mu - \frac{\kappa_\Theta}{2M_\Theta} \sigma_{\mu\nu} \partial^\nu \right] \gamma_5 \Theta A^\mu. \quad (14)$$

The interaction Lagrangians for a negative parity state to the pseudoscalar and pseudovector couplings are of the forms;

$$\begin{aligned} \mathcal{L}_{KN\Theta}^{PS} &= -ig_{KN\Theta} \bar{\Theta} N K, \\ \mathcal{L}_{KN\Theta}^{PV} &= -\frac{g_{KN\Theta}}{M - M_\Theta} \bar{\Theta} \gamma^\mu N \partial_\mu K, \end{aligned} \quad (15)$$

which are equivalent to each other for the free baryons. It must be noted, however, that they are slightly different from each other when, reduced to the non-relativistic spinor forms at threshold, i.e.,

$$\begin{aligned} \mathcal{L}_{KN\Theta}^{PS} &= -ig_{KN\Theta} \chi_\Theta^\dagger \chi_N K + \dots, \\ \mathcal{L}_{KN\Theta}^{PV} &= -ig_{KN\Theta} \frac{m_K}{M - M_\Theta} \chi_\Theta^\dagger \chi_N K + \dots. \end{aligned} \quad (16)$$

The difference is by the factor $\frac{m_K}{M - M_\Theta} \simeq 0.85$, which makes the PV coupling version somewhat smaller than the PS one by the factor of 0.85. The PV coupling Born amplitude for negative parity Θ^+ photoproduction can be derived by using the Lagrangians in Eqs.(14) and (15) for the coupling vertices relevant to the interaction diagrams shown in Fig. 1, which leads to replace the final state $\bar{u}_\Theta \rightarrow -\bar{u}_\Theta \gamma_5$ at every $KN\Theta$ vertex and u-channel propagator of Θ^+ , $S_F(p' - k) \rightarrow -\gamma_5 S_F(p' - k) \gamma_5$ in the amplitude Eq.(1), i.e.,

$$\mathcal{M}_{Born} = \mathcal{M}_{PV-pole} + \mathcal{M}_{KR} + \mathcal{M}_c, \quad (17)$$

where

$$\begin{aligned} \mathcal{M}_{PV-pole} &= \frac{eg_{KN\Theta}}{M - M_\Theta} \bar{u}_\Theta(p') \left\{ -F_1(s) \not{q} \frac{(\not{p}' + \not{k} + M)}{s - M^2} [Q_N \not{\epsilon} + i \frac{\kappa_N}{2M} \sigma^{\mu\nu} \epsilon_\mu k_\nu] + [-Q_\Theta \not{\epsilon} + i \frac{\kappa_\Theta}{2M_\Theta} \sigma^{\mu\nu} \epsilon_\mu k_\nu] \right. \\ &\quad \times \frac{(\not{p}' - \not{k} + M_\Theta)}{u - M_\Theta^2} \not{q} F_2(u) - Q_K F_3(t) \frac{(M - M_\Theta)(2q - k) \cdot \epsilon}{t - m_K^2} \left. \right\} u_N(p), \end{aligned} \quad (18)$$

$$\mathcal{M}_{KR} = \frac{eg_{KN\Theta}}{M - M_\Theta} \bar{u}_\Theta(p') \left\{ F_1(s) Q_N - Q_\Theta F_2(u) \right\} \not{\epsilon} u_N(p), \quad (19)$$

$$\begin{aligned} \mathcal{M}_c = & eg_{KN\Theta} \bar{u}_\Theta(p') \left\{ (F_1(s) - \hat{F}) Q_N \frac{(2p+k) \cdot \epsilon}{s - M^2} + Q_\Theta (F_2(u) - \hat{F}) \frac{(2p' - k) \cdot \epsilon}{u - M_\Theta^2} \right. \\ & \left. + Q_K (F_3(t) - \hat{F}) \frac{(2q - k) \cdot \epsilon}{t - m_K^2} \right\} u_N(p). \end{aligned} \quad (20)$$

By the similar procedure, the PS coupling Born amplitude from Eq.(8) is given by,

$$\mathcal{M}_{Born} = \mathcal{M}_{PS-pole} + \mathcal{M}_c, \quad (21)$$

where the contact interaction term \mathcal{M}_c is given by the same Eq.(20) and

$$\begin{aligned} & \mathcal{M}_{PS-pole} \\ = & eg_{KN\Theta} \bar{u}_\Theta(p') \left\{ -F_1(s) \frac{(\not{p} + \not{k} + M)}{s - M^2} [Q_N \not{\epsilon} + i \frac{\kappa_N}{2M} \sigma^{\mu\nu} \epsilon_\mu k_\nu] + [-Q_\Theta \not{\epsilon} + i \frac{\kappa_\Theta}{2M_\Theta} \sigma^{\mu\nu} \epsilon_\mu k_\nu] \right. \\ & \left. \times \frac{(\not{p}' - \not{k} + M_\Theta)}{u - M_\Theta^2} F_2(u) - Q_K F_3(t) \frac{(2q - k) \cdot \epsilon}{t - m_K^2} \right\} u_N(p). \end{aligned} \quad (22)$$

For an application of the K^* and K_1 exchanges in the t-channel, we use the transition amplitudes which are obtained from those corresponding to positive parity Θ^+ cases, Eqs.(11) and (13) with \bar{u}_Θ replaced by $-\bar{u}_\Theta \gamma_5$ in the $K^* N \Theta$ and $K_1 N \Theta$ vertices.

The process for the negative parity Θ^+ production was considered in Refs. [35, 37, 38, 39] for the photon-neutron reaction and found to have smaller cross sections than the positive-parity Θ^+ production in most existing calculations. Such a large suppression can be understood from the consideration of possible dynamical reasons, as discussed in Ref. [35]. However, the main reason for this is because the adopted coupling constant $g_{KN\Theta} = 0.3$ taken from the decay width less than 5 MeV, for instance in Ref. [38], is by a factor of $\frac{1}{7}$ smaller than that of positive parity. This reduction is of course reflected in the suppression of cross sections roughly by an order of magnitude, which are far below the observed one in the SAPHIR experiment. Thus, for this reason one may well doubt the possibility of negative parity state of Θ^+ . However, let us consider the decay width of the transition, $\Theta^+(\frac{1}{2}^\pm) \rightarrow KN(\frac{1}{2}^+)$ with both parities retained,

$$\Gamma_{\Theta(\frac{1}{2}^\pm)} = \frac{g_{KN\Theta}^2}{2\pi} \frac{|\mathbf{q}|}{M_\Theta} [\sqrt{M^2 + |\mathbf{q}|^2} \mp M], \quad (23)$$

and suppose that the coupling constant $g_{KN\Theta}$ is *a priori* given and the kaon momentum $|\mathbf{q}|$ in the Θ^+ rest frame is small. Then, the Eq.(23) implies that the width Γ_Θ would be small for the positive parity Θ^+ by taking the subtraction of nucleon mass from its energy inside bracket, and vice versa for negative parity. This means that the decay of positive parity is kinematically forbidden for small momentum. Therefore, Eq.(23) can be considered as a sort of selection rule for parity conservation in the sense that initially a negative parity state of Θ^+ is more likely to

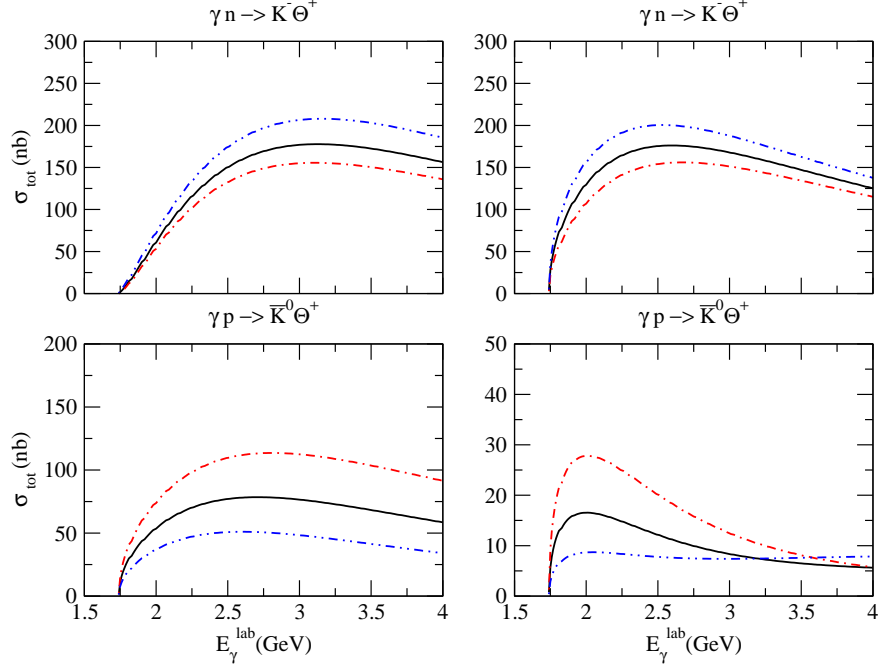


FIG. 7: Cross sections for $\gamma n \rightarrow K^- \Theta^+$ of PV(upper left panel) and PS scheme(upper right panel). Cross sections for $\gamma p \rightarrow \bar{K}^0 \Theta^+$ of PV(lower left panel) and PS scheme(lower right panel). The subtraction function (6) and form factors (7) with cutoff $\Lambda = 1.8$ GeV used. The solid lines are the results of Born amplitude with $g_{KN\Theta} = 0.7$, $\kappa_\Theta = 0$ when Θ^+ has negative parity. The dot-dashed lines with $\kappa_\Theta = 0.5$ and the dot-dot-dashed lines with $\kappa_\Theta = -0.5$. The maximum values κ_Θ are deduced from the application of ratio $\mu_{\Lambda(1116)}/\mu_{\Lambda(1405)}$ to $\kappa_{\Theta(+)}/\kappa_{\Theta(-)}$ with $\kappa_{\Theta(+)} = \pm 0.7$ of positive parity Θ^+ baryon.

decay to the final nucleon and kaon. That is, for a given coupling constant, the decay width Γ_Θ of negative parity should be larger than that of positive parity Θ^+ transition. For this reason, we adopt $g_{KN\Theta} = 0.7$ for the negative parity Θ^+ , taking an allowed upper limit of $\Gamma_\Theta < 25$ MeV.

Using the Born amplitude Eq.(17) for PV and Eq.(21) for PS scheme of negative parity Θ^+ photoproduction with $g_{KN\Theta} = 0.7$, the cross sections for the negative parity Θ^+ production are obtained and presented in Fig. 7. The results show that the total cross sections with Born contribution alone are already comparable to those observed in the SAPHIR experiment in both cases of PV and PS schemes for $\gamma n \rightarrow K^- \Theta^+$, although the coupling constant $g_{KN\Theta}$ is reduced to 30 %. On the other hand, the role of Θ^+ magnetic interaction, κ_Θ , is also sizable. The cross sections depend on κ_Θ nontrivially even with the small values ± 0.5 we assumed and this feature is independent of the two coupling schemes. In comparison with $\gamma n \rightarrow K^- \Theta^+$, the cross sections of $\gamma p \rightarrow \bar{K}^0 \Theta^+$ are sensitive to the sign of κ_Θ , changing half the amount of Born contribution to the cross sections, as shown in Fig. 7. The contribution of κ_Θ with positive sign enhances the cross

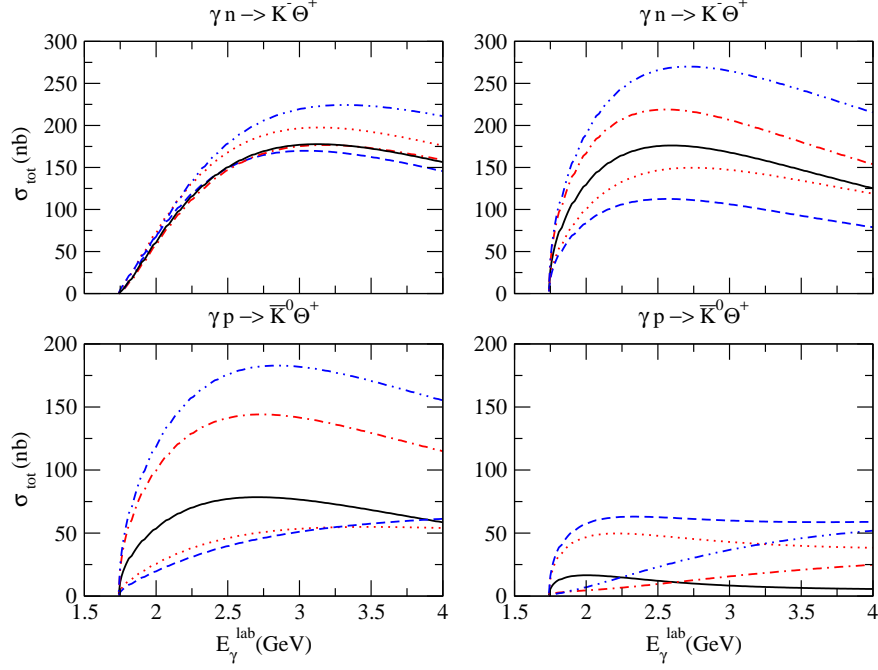


FIG. 8: Cross sections for $\gamma n \rightarrow K^- \Theta^+$ of PV(upper left) and PS scheme(upper right). Cross sections for $\gamma p \rightarrow \bar{K}^0 \Theta^+$ of PV(lower left) and PS scheme(lower right) when the Θ^+ has negative parity. The subtraction function (6) and form factors (7) with $\Lambda = 1.8$ GeV are used. $\kappa_\Theta = 0$ in any cases for all panels. The solid lines are the contribution of Born amplitude with $g_{KN\Theta} = 0.69$, $g_{K^*N\Theta} = 0$. The dot lines are the sum of Born amplitude and K^* with $g_{K^*N\Theta} = 0.42$. The dot-dashed lines the sum of Born amplitude and K^* with $g_{K^*N\Theta} = -0.42$. The dashed lines are the sum in total of Born terms, K^* and K_1 with $g_{K^*N\Theta} = 0.42$, $g_{K_1N\Theta} = -0.26$ for $\gamma n \rightarrow \bar{K}^0 \Theta^+$ and $g_{K_1N\Theta} = -0.38$ for $\gamma p \rightarrow \bar{K}^0 \Theta^+$ respectively. The dot-dot-dashed lines are the sum in total of Born, K^* and K_1 with $g_{K^*N\Theta} = -1.32$, $g_{K_1N\Theta} = +0.26$ for $\gamma n \rightarrow \bar{K}^0 \Theta^+$ and $g_{K_1N\Theta} = +0.38$ for $\gamma p \rightarrow \bar{K}^0 \Theta^+$ respectively.

section of $\gamma p \rightarrow \bar{K}^0 \Theta^+$ up to 130 nb in the case of PV scheme. Again we notice from these figures that the reaction $\gamma n \rightarrow K^- \Theta^+$ is dominant over the reaction $\gamma p \rightarrow \bar{K}^0 \Theta^+$ in the magnitude of total cross sections.

Next, we consider the contributions of K^* and K_1 exchanges to these processes. Fig. 8 illustrates the results when the K^* and K_1 contributions are included in the cross sections. Given the same values of the $K^* K \gamma$ and $K_1 K \gamma$ coupling constants as those of positive parity production, we adopt the coupling constant $g_{K^*N\Theta} = 0.18$ for negative parity Θ^+ coupling from the ratio $g_{K^*N\Theta}/g_{KN\Theta} = 0.6$, as has been done in the case of positive parity productions. The coupling constant $g_{K_1N\Theta}$ is determined from the assumption that the ratio $g_{K^*K\gamma}g_{K^*p\Lambda(1405)}/g_{K_1K\gamma}g_{K_1p\Lambda(1405)} \simeq -0.7$ extracted from the WJC model of kaon electromagnetic production [57] holds for the present coupling ratio $g_{K^*K\gamma}g_{K^*N\Theta}/g_{K_1K\gamma}g_{K_1N\Theta}$ as well. The results are shown in Fig. 8. In these figures, we find that

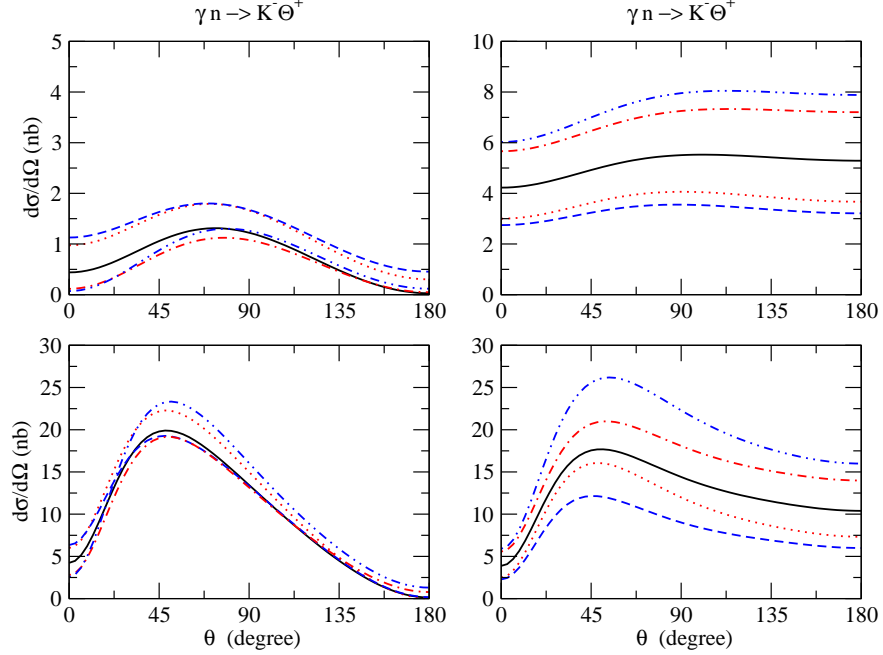


FIG. 9: Photoproduction angular distributions for $\gamma n \rightarrow K^- \Theta^+$ at $E_\gamma = 1.8$ GeV(upper left), $E_\gamma = 2.5$ GeV(lower left) of PV and $E_\gamma = 1.8$ GeV(upper right), $E_\gamma = 2.5$ GeV(lower right) of PS scheme with the negative parity Θ^+ . The notations are the same as in Fig. 8

the K^* and K_1 contributions are appreciable, in particular, with the large contribution from K_1 to $\gamma n \rightarrow K^- \Theta^+$ in the PS scheme and to $\gamma p \rightarrow \bar{K}^0 \Theta^+$ in the PV coupling scheme. This shows that the role of K_1 is important in the negative parity Θ^+ photoproduction. In fact, this feature can be anticipated from the analogous K^* dominance in the positive parity production, since the parities of K^* and K_1 are opposite to each other. It should be noted that the results of Fig. 8 are obtained with $\kappa_\Theta = 0$. The inclusion of magnetic moment, κ_Θ , gives additional 20 % increment of cross sections, if $\kappa_\Theta = 0.5$ taken. Therefore, with more residual interactions possible from the background of these processes as considered in Refs. [36, 37, 40], we confirm that the cross sections for $\gamma n \rightarrow K^- \Theta^+$ of both coupling schemes and also possibly the cross section for $\gamma p \rightarrow \bar{K}^0 \Theta^+$ of PV coupling at least are consistent with the observation in the SAPHIR experiment, although the model prediction for the cross section of $\gamma p \rightarrow \bar{K}^0 \Theta^+$ depends remarkably on the coupling scheme as shown in Fig. 8. In this regard, our result is contrary to the claim that the cross section for the negative parity Θ^+ is suppressed in comparison with the positive parity Θ^+ in the case of photoproduction [35, 36, 38, 39]. Analyzing only the total cross sections does not seem to provide a decisive conclusion on the parity of Θ^+ .

The angular distributions for $\gamma n \rightarrow K^- \Theta^+$ are displayed in Fig. 9 and for $\gamma p \rightarrow \bar{K}^0 \Theta^+$ in Fig.

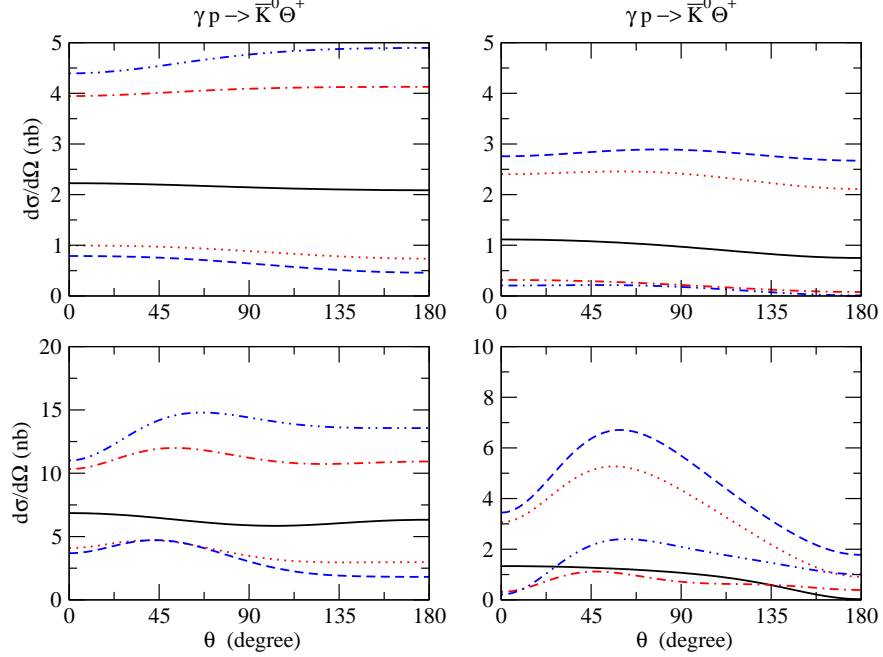


FIG. 10: Photoproduction angular distributions for $\gamma p \rightarrow \bar{K}^0 \Theta^+$ at $E_\gamma = 1.8$ GeV (upper left), $E_\gamma = 2.5$ GeV (lower left) of PV and $E_\gamma = 1.8$ GeV (upper right), $E_\gamma = 2.5$ GeV (lower right) of PS scheme with the negative parity Θ^+ . The notations are the same as in Fig. 8

10, respectively. By the parity argument, the produced kaon is anticipated to be in the p-wave state near threshold when the produced Θ^+ has negative parity. Such a feature is well reproduced in $\gamma n \rightarrow K^- \Theta^+$, whereas it is less clear for $\gamma p \rightarrow \bar{K}^0 \Theta^+$, regardless of the PV or PS scheme. Note that the scales of the cross sections of $E_\gamma = 1.8$ GeV in the two schemes are different in Fig. 9. In particular, at photon energy $E_\gamma = 2.5$ GeV we observe a forward peak due to a coherent interference of Born term with K^* and K_1 at around 45° both in the two schemes in Fig. 9. The coherent peak of Born term at around 45° is understood due to the t-channel kaon pole dominance, whereas no sizeable contribution appears from the u-channel. In the case of $\gamma p \rightarrow \bar{K}^0 \Theta^+$ presented in Fig. 10, the apparent flat curves of Born contribution despite the p-wave production of kaon may be understood due to the destructive interference between the produced p-wave kaon with the u-channel Born contribution cancelling each other. Thus, without the t-channel kaon pole contribution, this feature again manifests the p-wave kaon production in $\gamma p \rightarrow \bar{K}^0 \Theta^+$. Therefore, the development of the angular distribution of the cross section in the latter process comes from the t-channel K^* and K_1 contributions as the photon energy increases.

Before closing this section, it should be remarked that the angular distribution of $\gamma n \rightarrow K^- \Theta^+$ and $\gamma p \rightarrow \bar{K}^0 \Theta^+$ near threshold in particular shows a clear distinction between the two opposite

parities of Θ^+ baryon. As we have demonstrated up to this point, near threshold where the orbital excitations of kaon other than $L = 0$ are presumably suppressed, the conservation of parity and angular momentum imposes a specified form in the shape of angular distribution of $\gamma N \rightarrow K\Theta^+$, depending on what parity state of the Θ^+ is. Therefore, the observation of the reaction near threshold can provide an unambiguous way to clarify the parity of the Θ^+ . The importance of using this sort of conservation laws near threshold was also emphasized in Ref. [59] similar to ours, but for the different reaction $pp \rightarrow \Sigma^+\Theta^+$. The reaction they suggested instead of Θ^+ photoproduction takes the advantage of giving more tight condition on the parity and angular momentum at the initial pp state. However, the photoproduction of Θ^+ has already been observed and seems to be closer to realize the situation in experiment with less effort than the reaction suggested in Ref [59].

IV. SUMMARY AND DISCUSSION

We investigated the possibility of using photon induced Θ^+ production, $\gamma n \rightarrow K^-\Theta^+$ and $\gamma p \rightarrow \bar{K}^0\Theta^+$ to discriminate the parity of Θ^+ baryon. The processes are calculated for two possible parity states of Θ^+ baryon using hadron model where the interaction of $KN\Theta$ vertex is considered in two versions of PV and PS coupling schemes. We adopt the broader basis of prescription for the gauge invariance based on the Ohta-Haberzettl method, as discussed in the study of $K^+\Lambda$ and $K^+\Sigma$ photoproductions [45, 46, 47]. The results for the total and differential cross sections are to a large extent different from those of previous calculations [35, 36, 38, 39]. We may summarize the differences as follows. (i) Not only for the positive parity Θ^+ production but also for the negative parity Θ^+ production, the Born contribution here is large enough to yield both cross sections to be consistent with the observed cross section of SAPHIR experiment. Our results show that the cross section of Θ^+ production from the neutron is on the whole larger than that of Θ^+ production from the proton. (ii) Using the empirical ratio of $\frac{g_{K^*\Lambda}}{g_{K_1\Lambda}}$ extracted from $K^+\Lambda$ electromagnetic production for the determination of the coupling constants, $g_{K^*N\Theta}$ and $g_{K_1N\Theta}$, we obtain the K^* and K_1 contributions that are not overdominating compared to the Born contribution in the total cross sections as presented in Ref. [38]. This point is plausible from the correspondence of the present processes to the $\gamma n \rightarrow \pi^-p$ and $\gamma p \rightarrow \pi^0p$ where the contributions of vector meson $\rho(\omega)$ are about 10 % of the Born contribution at best to the threshold amplitude [51]. Furthermore, it is noticeable that the axial vector meson K_1 plays an important role in the negative parity Θ^+ production from the proton just like the role of K^* in the positive parity Θ^+ production from the

proton. (iii) It may be premature to discard the negative parity Θ^+ production using only such minimal models that contain Born terms with one or two more t-channel meson exchanges whose coupling constants and cutoff parameter Λ are not even known. Our results indicate that the possibility of negative parity Θ^+ photoproduction cannot be ruled out at least within the present framework of hadronic model. (iv) Finally we find that the angular distributions of the production processes for the two opposite parity states are clearly distinct from each other as we demonstrated. Therefore, we suggest that the observation of angular distribution in the photoproduction process can serve as a more useful tool to distinguish the parity of Θ^+ baryon compared to just the measurement of total cross sections.

Acknowledgments

This work was supported in part by 2003 Hankuk Aviation university Faculty Research Grant and in part by a grant from the U.S. Department of Energy (DE-FG02-96ER 40947).

-
- [1] LEPS Collaboration, T. Nakano *et al.*, Phys. Rev. Lett. **91**, 012002 (2003).
 - [2] SAPHIR Collaboration, J. Barth *et al.*, Phys. Lett. B **572**, 127 (2003).
 - [3] CLAS Collaboration, S. Stepanyan *et al.*, hep-ex/0307018.
 - [4] DIANA Collaboration, V. V. Barmin *et al.*, hep-ex/0304040.
 - [5] A. E. Asratyan, A. G. Dolgolenko, and M. A. Kubantsev, hep-ex/0309042.
 - [6] D. Diakonov, V. Petrov, and M. Polyakov, Z. Phys. A **359**, 305 (1997).
 - [7] H. Weigel, Eur. Phys. J. A **2**, 391 (1998).
 - [8] M. Chemtob, Nucl. Phys. **B256**, 600 (1985).
 - [9] M. Przaszłowicz, hep-ph/0308114.
 - [10] R. L. Jaffe and F. Wilczek, hep-ph/0307341.
 - [11] R. L. Jaffe, Phys. Rev. D **15**, 267 (1977); Phys. Rev. D **15**, 281 (1977).
 - [12] K. Cheung hep-ph/0308176.
 - [13] Fl. Stancu and D. O. Riska, Phys. Lett. B **575**, 242 (2003).
 - [14] C. E. Carlson, C. D. Carone, H. J. Kwee, and V. Nazaryan, Phys. Lett. B **573**, 101 (2003); hep-ph/0310038.
 - [15] L. Ya. Golzman, Phys. Lett. B **575**, 18 (2003); hep-ph/0309092.
 - [16] R. A. Williams and P. Guèye, nucl-th/0308058.
 - [17] M. karliner and H. J. Lipkin, Phys. Lett. B **575**, 249 (2003).
 - [18] E. Shuryak and I. Zahed, hep-ph/0310270.

- [19] H. Walliser and V. B. Kopeliovich, hep-ph/0304058.
- [20] B. K. Jennings and K. Maltman, hep-ph/0308286.
- [21] D. Borisyuk, M. Faber, and A. Kobushkin, hep-ph/0307370.
- [22] N. Itzhaki, I. R. Klebanov, P. Ouyang, and L. Rastelli, hep-ph/0309305.
- [23] B. Wu and B.-Q. Ma, hep-ph/0311331.
- [24] S.-L. Zhu, Phys. Rev. Lett. **91**, 232002 (2003).
- [25] R. D. Matheus, F. S. Navarra, M. Nielsen, R. da Silva, and S. H. Lee, hep-ph/0309001.
- [26] J. Sugiyama, T. Doi, and M. Oka, hep-ph/0309271.
- [27] A. Hosaka, Phys. Lett. B **571**, 55 (2003).
- [28] T. D. Cohen, hep-ph/0309111; T. D. Cohen and R. F. Lebed, hep-ph/0309150.
- [29] F. Csikor, Z. Fodor, S. D. Katz, and T. G. Kovács, hep-lat/0309090.
- [30] S. Sasaki, hep-lat/0310014.
- [31] B. G. Wybourne, hep-ph/0307170.
- [32] R. Bijker, M. M. Giannini, and E. Santopinto hep-ph/0310281.
- [33] J. Randrup, Phys. Rev. C **68**, 031903 (2003).
- [34] L. W. Chen, V. Greco, C. M. Ko, S. H. Lee, and W. Liu nucl-th/0308006.
- [35] S. I. Nam, A. Hosaka, and H.-C. Kim, hep-ph/0308313.
- [36] W. Liu and C. M. Ko, Phys. Rev C **68**, 045203 (2003); nucl-th/0309023.
- [37] W. Liu and C. M. Ko, nucl-th/0310087.
- [38] Y. S. Oh, H. C. Kim, and S.-H. Lee, hep-ph/0310019.
- [39] Q. Zhao and J. S. Al-Khalili, hep-ph/0310350.
- [40] K. Nakayama and K. Tsushima, hep-ph/0311112.
- [41] S. Janssen, J. Ryckebusch, D. Debruyne, and T. Van Cauteren, Phys. Rev. C **65**, 015201 (2001).
- [42] S. Janssen, J. Ryckebusch, W. Van Nespén, D. Debruyne, and T. Van Cauteren, Eur. Phys. J. A **9**, 115 (2000).
- [43] C. Bennhold, T. Mart, A. Waluyo, H. Haberzettl, G. Penner, T. Feuster, and U. Mosel, nucl-th/9901066.
- [44] T. Mart, S. Sumowidagdo, C. Bennhold, and H. Haberzettl, nucl-th/0002036.
- [45] K. Ohta, Phys. Rev. C **40**, 1335 (1989); Phys. Rev. C **46**, 2519 (1992).
- [46] H. Haberzettl, Phys. Rev. C **56**, 2041 (1997). H. Haberzettl *et al.*, nucl-th/9804051. H. Haberzettl, Phys. Rev. C **62**, 034605 (2000).
- [47] H. Haberzettl, C. Bennhold, T. Mart, and T. Feuster, Phys. Rev. C **58**, R40 (1998).
- [48] R. M. Davidson and R. Workman, nucl-th/0101066; nucl-th/0102046.
- [49] Y. S. Oh, H. C. Kim, and S. H. Lee, hep-ph/0310117.
- [50] D. Diakonov and V. Petrov, hep-ph/0310212.
- [51] D. Drechsel and L. Tiator, J. Phys. G: Nucl. Part. Phys. **18**, 449 (1992).
- [52] O. Hanstein, D. Drechsel, and L. Tiator, nucl-th/9709067.
- [53] M. Fuchs *et al.*, Phys. Lett. B **368**, 20 (1996).

- [54] M. V. Polyakov and A. Rathke, hep-ph/0303138.
- [55] <http://pdg.lbl.gov/pdg.html>
- [56] K. Haglin, Phys. Rev. C **50**, 1688 (1994).
- [57] R. A. Williams *et al.*, Phys. Rev. C **46**, 1617 (1992).
- [58] S. S. Hsiao, D. H. Lu, and S. N. Yang, Phys. Rev. C **61**, 068201 (2000).
- [59] A. W. Thomas, K. Hicks, and A. Hosaka, hep-ph/0312083.